







Impacts of native vegetation on the hydraulic properties of the concentrated flows in bank gullies


SU Zheng-an^{1*}  <http://orcid.org/0000-0002-7505-8739>;  e-mail: suzhengan@imde.ac.cn


HE Zhou-yao^{1,2}  <https://orcid.org/0000-0001-7032-4535>; e-mail: 1062061514@qq.com


ZHOU Tao^{1,3}  <https://orcid.org/0000-0001-5040-8571>; e-mail: 1712815401@qq.com


WANG Jun-jie^{1,3}  <https://orcid.org/0000-0001-8115-5247>; e-mail: 1045455627@qq.com


WANG Xiao-yi^{1,4}  <https://orcid.org/0000-0002-2268-0276>; e-mail: 14181692@qq.com

WANG Li-juan^{1,3}  <https://orcid.org/0000-0002-6394-5306>; e-mail: 2679833673@qq.com

FANG Hai-dong⁵  <https://orcid.org/0000-0003-0372-7048>; e-mail: 406373828@qq.com

SHI Liang-tao⁵  <https://orcid.org/0000-0002-0038-9250>; e-mail: 282547489@qq.com

LIU Yi-han^{1,6}  <https://orcid.org/0000-0003-3074-0926>; e-mail: 1026147047@qq.com

WU Zuo^{1,4}  <https://orcid.org/0000-0002-5363-300x>; e-mail: xxxwuzuo.com@qq.com

*Corresponding author

¹ Key Laboratory of Mountain Surface Processes and Ecological Regulation, Institute of Mountain Hazards and Environment, Chinese Academy of Sciences, Chengdu 610041, China

² Forestry College, Sichuan Agricultural University, Chengdu 611130, China

³ University of Chinese Academy of Sciences, Beijing 100049, China

⁴ College of Water Conservancy and Hydropower Engineering, Sichuan Agricultural University, Ya'an 625014, China

⁵ Institute of Tropical Eco-agricultural Sciences, Yunnan Academy of Agricultural Sciences, Yuanmou 651300, China

⁶ College of Geography and Resources Science, Sichuan Normal University, Chengdu 610101, China

Citation: Su ZA, He ZY, Zhou T, et al. (2021) Impacts of native vegetation on the hydraulic properties of the concentrated flows in bank gullies. *Journal of Mountain Science* 18(4). <https://doi.org/10.1007/s11629-020-6287-9>

© Science Press, Institute of Mountain Hazards and Environment, CAS and Springer-Verlag GmbH Germany, part of Springer Nature 2021

Abstract: To quantify the impacts of native vegetation on the spatial and temporal variations in hydraulic properties of bank gully concentrated flows, a series of in situ flume experiments in the bank gully were performed at the Yuanmou Gully Erosion and Collapse Experimental Station in the dry-hot valley region of the Jinsha River, Southwest China. This experiment involved upstream catchment areas with

one- and two-year native grass (*Heteropogon contortus*) and bare land drained to bare gully headcuts, i.e., Gullies 1, 2 and 3. In Gully 4, *Heteropogon contortus* and *Agave sisalana* were planted in the upstream catchment area and gully bed, respectively. Among these experiments, the sediment concentration in runoff in Gully 3 was the highest and that in Gully 2 was the lowest, clearly indicating that the sediment concentration in runoff obviously decreased and the deposition of sediment obviously increased as the vegetation cover increased. The

Received: 28-Jun-2020

Revised: 30-Sep-2020

Accepted: 08-Mar-2021

concentrated flows were turbulent in response to the flow discharge. The concentrated flows in the gully zones with native grass and bare land were sub- and supercritical, respectively. The flow rate and shear stress in Gully 3 upstream catchment area were highest among the four upstream catchment areas, while the flow rate and shear stress in the gully bed of Gully 4 were lowest among the four gully beds, indicating that native grass notably decreased the bank gully flow rate and shear stress. The Darcy–Weisbach friction factor (resistance f) and flow energy consumption in the gully bed of Gully 4 were notably higher than those in the other three gully beds, clearly indicating that native grass increased the bank gully surface resistance and flow energy consumption. The Reynolds number (Re), flow rate, shear stress, resistance f , and flow energy consumption in the gully beds and upstream areas increased over time, while the sediment concentration in runoff and Froude number (Fr) decreased. Overall, increasing vegetation cover in upstream catchment areas and downstream gully beds of the bank gully is essential for gully erosion mitigation.

Keywords: Soil erosion; Indigenous grass species; Bank gully; Concentrated flows; Flow energy consumption; Dry and hot valley.

1 Introduction

Gully erosion is a type of soil degradation that occurs in a wide variety of environments and has received much attention worldwide (Poesen et al. 2003; Valentin et al. 2005), including North America (Bennett and Casali 2001; Wells et al. 2010; Wilson 2011), Europe (Kirkby et al. 2003; Gómez Gutiérrez et al. 2009; Marzloff et al. 2011), Asia (Zhu 2012; Zakerinejad and Maerker 2015; Zabihi et al. 2018), Africa (Tebebu et al. 2010; Zegeye et al. 2018), and Oceania (Hancock and Evans 2010; Wilkinson et al. 2013; Shellberg et al. 2016). The gully plays an important role in generating and transferring soil sediment in a watershed (Poesen et al. 2003), reduces the available area of agricultural lands or grasslands in upstream catchments and increases sedimentation in downstream pond reservoirs, rivers or lakes (Su et al. 2014). To date, more attention has been given to ephemeral gullies, while few studies have focused on bank gullies.

Quantitative studies on gully erosion mainly began in the late 20th century, and many studies have

concentrated on gully erosion thresholds. Gully erosion is clearly a threshold phenomenon, and gully channels can only develop if the concentrated (overland) flow intensity during a rain event exceeds the threshold value (Horton 1945; Vandekerckhove et al. 1998; Poesen et al. 2003). After the concept of the threshold force required for channel initiation was first proposed by Horton (1945), soil scientists assessed critical environmental conditions for gully erosion in terms of rainfall, topography, soil type (or lithology) and land use (Poesen et al. 2003). In particular, many studies have focused on the topographic threshold concept for gully initiation by establishing critical S – A relations for incipient permanent and ephemeral gully erosion in a range of different environments (Vandekerckhove et al. 1998; Hancock and Evans 2006; Dong et al. 2013; Gudino-Elizondo et al. 2018). Moreover, several studies have been conducted to better understand the hydrodynamic process of gully erosion using scouring experiments of concentrated flows (Su et al. 2015a; Wells et al. 2016; Zhang et al. 2018; Dong et al. 2019). Notably, few studies have focused on the temporal and spatial variations in gully erosion processes for different land use types.

Gully erosion studies are performed to reveal the mechanism of gully occurrence and development and propose innovative measures to control gully erosion. Compared to slope erosion research, innovations in gully erosion control research are rather limited (Valentin et al. 2005). Previous studies have proposed establishing grassed waterways or vegetation buffer strips to prevent gully development and check dams with drop structures in gullies (Nyssen et al. 2004; Pederson et al. 2006; Dong et al. 2018; Zegeye et al. 2018). In China, gully erosion control has been debated since the 1950s. Some soil scientists have advocated that more prevention measures should be implemented in upstream catchment areas where concentrated flows form, while other soil scientists have declared that more prevention measures should be implemented to headcut and channel gullies. The origin of the above debate was a lack of understanding of the erosion process and the hydrodynamic properties of gully erosion. In recent years, several ecological restoration projects, such as the Grain-to-Green project and Yangtze River shelterbelt project, have been conducted to improve soil erosion control in China (Fu et al. 2011). Under these conditions, establishing an ecological restoration model in a gully

erosion development region is crucial.

The dry-hot valley region is a particular ecologically vulnerable region in Southwest China. This region covers an area of approximately 1.2×10^4 km² and is well known for its dry and hot weather from October to April, when it is cold in most areas of China (Su et al. 2015b). The zonal vegetation type is tropical bushveld with scattered trees, resembling the tropical savanna ecosystem (Su et al. 2019). The gullies in this region are often large in scale with deep incisions, steep gully sidewalls and a mix of fluvial and lacustrine deposits in different soil layers (Dong et al. 2014; Su et al. 2015b). Gully erosion accounts for much of the total soil erosion and soil sediment of rivers, and the gully density in this region ranges from 3 to 5 km km⁻² (Su et al. 2014). However, compared to the large number of gully erosion studies in the Loess Plateau of China, few studies on the hydraulic properties and headward erosion process of gullies have been conducted in the dry-hot valley region of China (Chen et al. 2013; Su et al. 2015a).

Despite the importance of gully headward erosion in the dry-hot valley region of China, limited data are available on the impacts of native vegetation on the erosion rate and hydraulic properties of bank

gullies. Therefore, this study investigates gully heads in the field to quantify the impacts of native vegetation (i.e., *Heteropogon contortus* and *Agave sisalana*) on the spatial and temporal variations in the erosion rate and hydraulic properties of the concentrated flows at the bank gullies in the dry-hot valley region of Southwest China.

2 Material and Methods

2.1 Study area

Experiments were carried out at the Yuanmou Gully Erosion and Collapse Experimental Station (25°23' N to 26°06' N, 101°35' E to 102°06' E) in Yuanmou County (Fig. 1), Yunnan Province, China, which belongs to the dry-hot valley of the Jinsha River (Su et al. 2015a). The erosive rainfall was mainly distributed from June to October, and the rainfall days ranged from 78 to 90 d (Table 1). Annual precipitation was recorded from 474.42 to 738.19, with a mean annual precipitation of 625.62 mm from 2014 to 2018. The mean annual potential evaporation was 3847.80 mm, indicating that the total

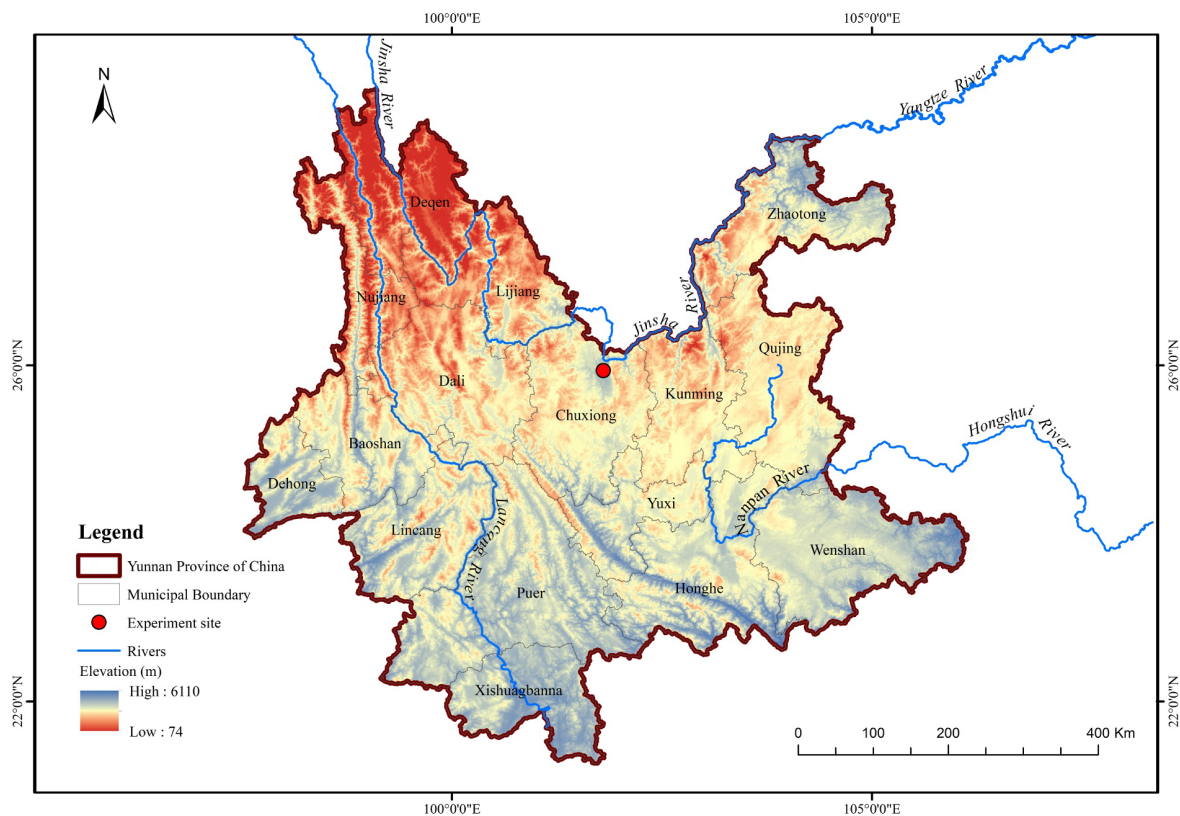


Fig. 1 Study area in Yuanmou County, Yunnan Province, China.

Table 1 Rainfall temporal distribution in the study area

Month	Year 2014		Year 2015		Year 2016		Year 2017		Year 2018	
	Rainfall (mm)	Rainfall days (d)	Rainfall (mm)	Rainfall days (d)	Rainfall (mm)	Rainfall days (d)	Rainfall (mm)	Rainfall days (d)	Rainfall (mm)	Rainfall days (d)
January	5.80	3	56.40	7	0.00	0	7.2	4	13.20	4
February	2.20	3	0.20	1	10.40	4	0.2	1	3.55	2
March	1.60	2	34.60	2	0.60	1	14.8	4	7.62	2
April	0.20	1	17.60	5	1.20	2	35.4	8	2.77	3
May	6.20	3	13.40	3	9.14	3	31.4	6	158.6	17
June	120.40	15	57.80	8	81.90	11	106.4	12	123.89	13
July	230.00	22	119.00	20	205.97	16	326.2	24	68.55	11
August	109.20	11	211.00	18	102.50	14	68.4	16	91.49	16
September	66.00	7	54.80	7	235.38	17	59.8	6	1.75	7
October	31.40	7	70.20	7	57.86	10	25.2	8	3.00	9
November	8.40	2	9.20	2	29.44	4	0.25	1	/	/
December	8.00	2	6.60	5	3.80	2	0	0	/	/
Total	589.40	78	650.80	85	738.19	84	675.27	90	474.42	84

evaporation was 6.0 times higher than the total precipitation (Su et al. 2014). The temperature ranged from 0.1°C to 42°C, with a mean annual temperature of 21.8°C (Su et al. 2015a). Dry red soil, which was classified as a Ustic Ferrisol in the Chinese Taxonomy and a Ferralic Cambisol in the FAO soil taxonomic system (FAO 2015), was the dominant soil type. The bulk density of the dry red soil ranged from 1.4 to 1.8 g cm⁻³ (Su et al. 2015b). The soil erosion rate, which was dominated by gully erosion, was estimated at 1.64×10⁴ t km⁻² yr⁻¹ in this region (Su et al. 2014). Accordingly, this area is considered a typical ecologically fragile zone in the mountainous region of Southwest China due to the extreme climate and serious soil erosion occurring (Dong et al. 2014). The dominant vegetation types in this area were herbaceous plants and sparsely dispersed shrubs due to dry-hot weather conditions (Dong et al. 2019). *Heteropogon contortus*, which is a local species that can grow rapidly under drought and hot environmental conditions, is the most common grass growing in the study area (Dong et al. 2018). *Agave sisalana* is also a common grass in the dry-hot valley region of Southwest China.

2.2 Experimental procedure

The background field information and the experimental platforms have been described in Su et al. (2014, 2015). In summary, a typical in situ bank gully (10.5 m wide with a 6-m long downstream gully bed and a 0.7-m high headcut) and a 12-m long upstream catchment area were selected as scouring experimental sites (Fig. 2) (Su et al. 2014). This bank gully and its upstream catchment area were divided

into four experimental platforms of similar dimensions (each platform was 2 m wide, and the distance between two platforms was 0.5 m) from which straight headcuts were constructed (hereafter referred to as Gullies 1 to 4) (Su et al. 2014). The slope lengths of the upstream catchment area and gully bed were 12 m and 6 m with mean slope gradients of 7.5° and 20°, respectively, and the height of the vertical headcut was 0.7 m (Su et al. 2015a).

The soil bulk density ranged from 1.60 to 1.64 g cm⁻³. The soil texture was sandy loam, and the soil particle size fractions were approximately 63% sand, 24% silt, 13% clay and 72% sand, 20% silt, and 8% clay in the upstream catchment area and the

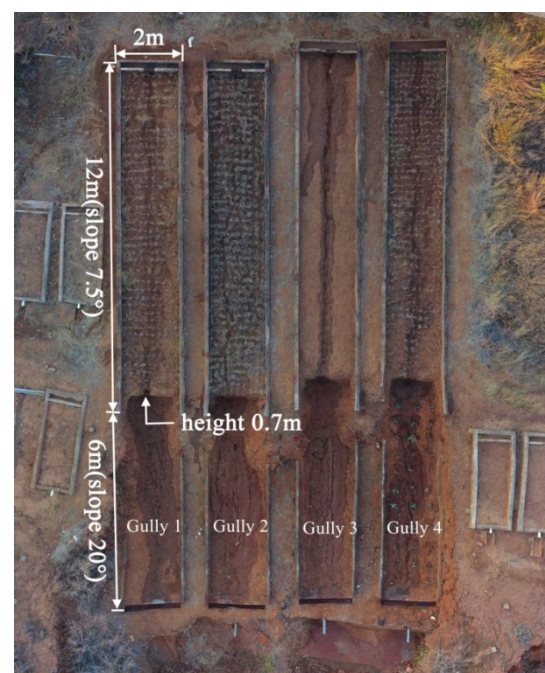


Fig. 2 Experimental plots of this study.

downstream gully beds, respectively (Su et al. 2015a).

Heteropogon contortus and *Agave sisalana*, the dominant indigenous species in the study area, were selected for this experiment. *Heteropogon contortus* and *Agave sisalana* were planted by hole sowing in the upstream catchment area and gully bed, respectively (Table 2). In Gully 1, one-year *Heteropogon contortus* and bare land were set in the upstream catchment area and gully bed, respectively. In Gully 2, two-year *Heteropogon contortus* and bare land were set in the upstream catchment area and gully bed, respectively. Gully 3 was set as the blank experimental platform with bare land in the upstream catchment area and in the gully bed. In Gully 4, to explore different vegetation restoration models, one-year *Heteropogon contortus* and *Agave sisalana* were planted in the upstream catchment area and gully bed, respectively. The coverage ranged from 30% to 40% for the upstream catchment area of Gully 1 and gully 4, while the coverage ranged from 70% to 80% for the upstream catchment area of Gully 2. The coverage ranged from 10% to 20% for the gully bed of gully 4. Meanwhile, no plowing, harrowing or fertilizing practices were conducted in those plots, while irrigation practice was conducted in the first year to ensure survival of the native grass.

A series of 120-min scouring tests with a flow discharge of 90 L min⁻¹, which were used to simulate concentrated flows in bank gullies under rainstorms, were performed in the bank gully experiment platform in January 2019 (dry season) (Fig.2). The flow discharge was determined by the average precipitation of heavy rainfall events and the drainage area in this region proposed by previous studies (Dong et al. 2013, 2018). We initially pumped water into a current stabilizer consisting of a three-way pipe and equalization pond to maintain a stable discharge, and then water was transported to a flow metre to measure flow discharge and a water storage groove with a V-shaped export above the middle of the upstream catchment area to conduct the concentrated flow scouring experiment (Su et al. 2015a).

Table 2 Experimental settings in this study

Item	Gully 1		Gully 2		Gully 3		Gully 4	
	Drainage area	Gully bed	Drainage area	Gully bed	Drainage area	Gully bed	Drainage area	Gully bed
Width (m)	2	2	2	2	2	2	2	2
Length (m)	12	6	12	6	12	6	12	6
Measures	1-year <i>Heteropogon contortus</i>	Bare land	2-year <i>Heteropogon contortus</i>	Bare land	Bare land	Bare land	1-year <i>Heteropogon contortus</i>	1-year <i>Agave sisalana</i>

Six hydraulic observational sections were set at 2, 4, 6, 8, 10, and 12 m in the downslope direction of the upstream catchment area, and three hydraulic observational sections were set at 14, 16, and 18 m in the downslope direction of the downstream gully bed, as in previous studies (Su et al. 2015a). The headcut included the area between the upper scarp edge and the scour hole at the summit of the gully bed (Su et al. 2015b). We measured hydraulic parameters, such as flow velocity (v , m s⁻¹), surface width (w , m), depth (d , m), and temperature (T , °C), by using conventional methods. The colour tracer method was used to measure the flow velocity, while a ruler and tape were used to measure the flow width and depth (Su et al. 2015a). A centigrade thermometer was used to measure the flow temperature. The flow velocity, width, depth, and temperature were repeatedly measured every 10 min (Su et al. 2015a).

2.3 Sediment concentration

To reflect the temporal variation in soil loss, a mixture of overland flow and soil sediment was collected at the outlet of the experimental platforms using a 1000-mL plastic bottle at 1, 3, 5, 7 and 10 min at the initial stage, and the same mixture was collected at 5-min intervals after the initial 10 min. The sediment concentration in runoff was determined from the sediment mass and volume of sediment samples that were first precipitated with alum, followed by water decanting and then oven drying at 105°C (Dong et al. 2018).

2.4 Hydraulic parameters

The flow discharge (Q , L min⁻¹), Reynolds number (Re), Froude number (Fr), flow shear stress (τ , Pa), Darcy–Weisbach friction factor (f), and energy consumption (ΔE , J s⁻¹) were calculated using v , w , and d data as well as T . The equations are as follows (Su et al. 2015a):

$$R_e = vr / \eta \tag{1}$$

$$Fr = v / \sqrt{gd} \tag{2}$$

$$\tau = \gamma g r J \tag{3}$$

$$f = 8rJg / v^2 \tag{4}$$

where r is the hydraulic radius (m), $r=A/Wp$, A is the cross-sectional area, $A=w \times d$, Wp is the wetted perimeter (m), $Wp=w+2d$; η is the water kinematic viscosity coefficient ($m^2 s^{-1}$), $\eta=0.01775/(1+0.0337T+0.000221T^2)$ (Gong et al. 2011); g is the acceleration due to gravity ($m s^{-2}$); γ is the water density ($kg m^{-3}$); and J is the hydraulic gradient ($m m^{-1}$), which is calculated by the water slope.

The energy consumption (ΔE) is deduced by comparing the total energy (E_x) at the other slope positions to the kinetic energy (E_k) and potential energy (E_p) of the flow at the summit ($J s^{-1}$) as follows (Su et al. 2015a):

$$E_x = E_p + E_k - E_x = \gamma q g l \sin \partial + \gamma q v^2 / 2 - (q' \gamma v_x^2 / 2 + q' \gamma g (l - x) \sin \partial) \tag{5}$$

where q is the discharge at the summit slope ($m^3 m^{-1} s^{-1}$); l is the slope length (m); ∂ is the angle of the slope; q' is the discharge at the lower slope positions ($m^3 m^{-1} s^{-1}$); v_x is the velocity at the lower slope positions ($m s^{-1}$); and x is the distance from the summit slope (m).

If there were several runoff branches in some sections of the experimental plot, the flow hydraulic parameter was calculated as in previous studies (Dong et al. 2018, 2019).

2.5 Data analysis

A nonlinear regression analysis was conducted to determine the relationships between the sediment concentration in runoff (Appendix 1), infiltration rate, energy consumption of the flow (Appendix 2), and time using SPSS statistics 17.0 and SigmaPlot software (version 10.0).

3 Results

3.1 Changes in the erosion process

At the initial stages, the infiltration rate and runoff width were high, and the runoff radius was low (Fig. 3), which was similar to laminar flow. As the experiment progressed, concentrated flow gradually

occurred in the centre of the experiment platform, and shallow gullies appeared in the upstream catchments and downstream gully beds as the flow width decreased and the hydraulic radius increased (Fig. 2). Meanwhile, the soil infiltration rate decreased and reached a steady state. Additionally, in some sections, the runoff branched into two or three branches due to interception effects of native grass (Dong et al. 2018). At the gully wall, the concentrated flow separated as an attached wall jet and a free jet, and a washing hole was formed and gully headcut retreated due to the combined effects of the attached wall jet and free jet, which was similar to previous studies (Su et al. 2015a, b).

An exponential decreasing trend in the sediment concentration in runoff and a power decreasing trend in the soil infiltration rate were observed as the experiment progressed (Figs. 3 and 4; $P < 0.01$). It should be noted that a sudden increase in the sediment concentration in runoff might occur due to gully headcut collapse. In Gully 1, the sediment concentration in runoff at the initial stages (0-5 min) decreased from 200.59 to 87.66 $g L^{-1}$, and a steady state was attained after the 40-min scour experiment with an average sediment concentration in runoff of 5.50 $g L^{-1}$. In Gully 2, the sediment concentration in runoff at the initial stages (0-5 min) decreased from 122.36 to 53.71 $g L^{-1}$, and a steady state in the sediment concentration in runoff was attained after the 20-min scour experiment. A new steady state was attained after the 60-min scour experiment with the average sediment concentration in runoff of 2.99 $g L^{-1}$. In Gully 3, the sediment concentration in runoff at the initial stages (0-5 min) decreased from 410.27 to 282.01 $g L^{-1}$, and a steady state was attained after the 50-min scour experiment with an average sediment concentration of 6.09 $g L^{-1}$. In Gully 4, the sediment concentration in runoff at the initial stages (0-5 min) decreased from 165.16 to 116.08 $g L^{-1}$, and a steady state was observed after the 50-min scour experiment with a sediment concentration in runoff of 3.90 $g L^{-1}$. Meanwhile, a similar temporal variation in the soil infiltration rate could be found in those gullies, and the soil infiltration rates under steady state were higher in the gullies with native grass than in those gullies with bare land. These results indicated that native grass could substantially reduce the soil erosion rate and increase the soil infiltration rate. Additionally, those results showed a similar behaviour among Gullies 1, 2 and 4 for the generation of

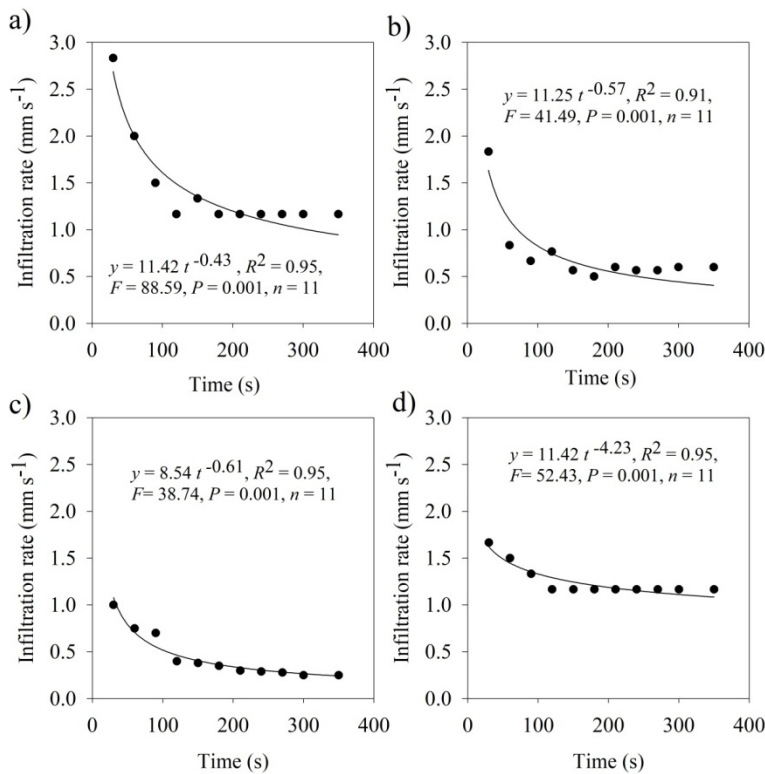


Fig. 3 Soil infiltration rate at the various gully positions in (a) the upstream catchment area of Gully 1; (b) upstream catchment area of Gully 3; (c) downstream gully beds of Gully 3; and (d) downstream gully beds of Gully 4.

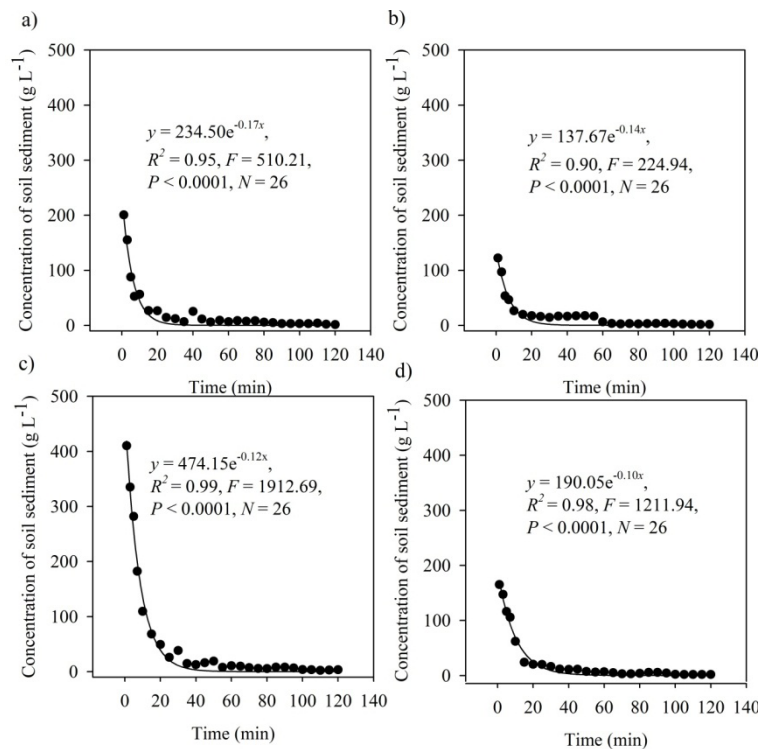


Fig. 4 Sediment concentration in runoff in each bank gully over time: (a) Gully 1; (b) Gully 2; (c) Gully 3 and (d) Gully 4.

sediments in the first 20 min due to negative grass.

3.2 Changes in the flow type

Open channel flows are turbulent for $Re \geq 1000$ and laminar for $Re < 1000$, while channel flows are supercritical for $Fr \geq 1$ and subcritical for $Fr < 1$ (Gong et al. 2011). Figs. 5 and 6 show the variations in Re and Fr in the upstream catchment areas and downstream gully beds, respectively, in the different native grass restoration models. The Re values in the upstream catchment areas and downstream gully beds greatly exceeded 1000, indicating that the overland flow in the downstream gully beds and the upstream catchment areas was turbulent (Su et al. 2015a). However, $Fr > 1$ was observed in the upstream catchment area of Gully 3 and in the downstream gully beds of Gullies 1, 2 and 3 with bare land, while $Fr < 1$ was observed in the upstream catchment area of Gullies 1, 2 and 4 and in the downstream gully bed of Gully 4 with native grass. These results indicated that the overland flows in the gully zones with bare land were supercritical, while the overland flows in the gully zones with the native grass treatments were subcritical.

As the experiment progressed, Re gradually increased, while Fr gradually decreased under those treatments. In the upstream catchment areas, Re and Fr in Gully 3 with bare land were notably higher than those in the other gullies with native grass. In the downstream gully beds, Re and Fr in Gully 4 with native grass were notably lower than those in the other gullies with bare land. No clear differences in Re and Fr were observed among the upstream catchment areas of Gullies 1, 2 and 4 with native grass and among the downstream gully beds of Gullies 1, 2 and 4 with bare land (Tables 3 and 4). In addition, following an initial period (60

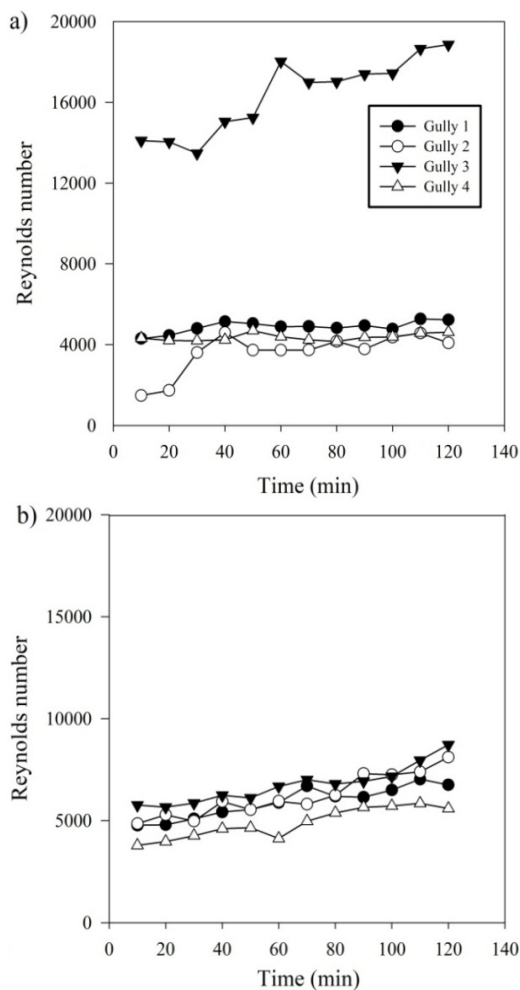


Fig. 5 Reynolds number at the various gully positions in (a) the upstream catchment areas and (b) downstream gully beds over time.

min) of adjustment, steady-state *Re* and *Fr* conditions were attained in each bank gully under the experimental conditions.

3.3 Changes in the flow rate and shear stress

Figs. 7 and 8 show the variations in the flow rate and flow shear stress, respectively, in Gullies 1-4. Except in Gully 3, the flow rate and flow shear stress in the upstream catchment areas were notably lower than those in the downstream gully beds in the other bank gullies. In Gully 3, the flow rate in the upstream catchment area was higher than that in the downstream gully beds, while the flow shear stress in the upstream catchment area was notably lower than that in the downstream gully beds. Moreover, the flow rate and flow shear stress in the upstream catchment area and downstream gully bed of Gully 3 with bare

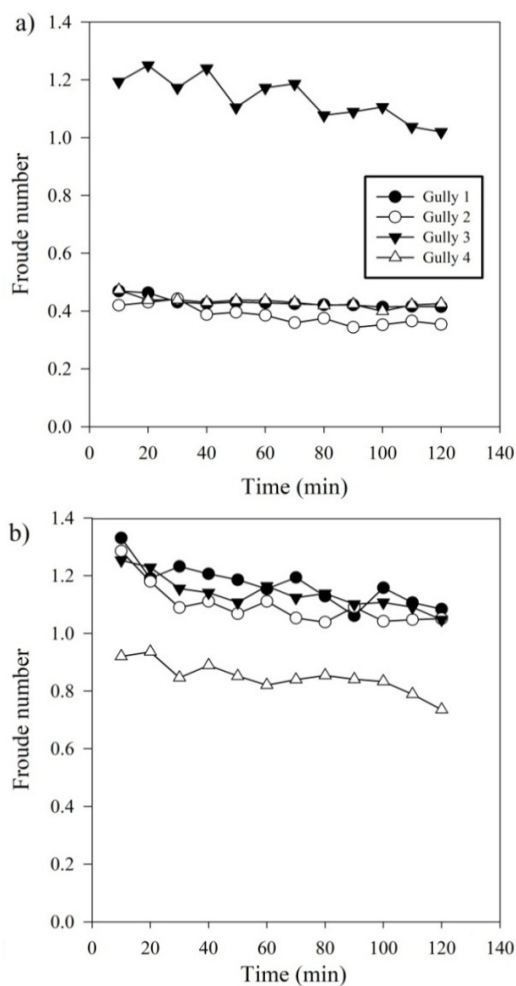


Fig. 6 Froude number at the various gully positions in (a) the upstream catchment areas and (b) downstream gully beds over time.

land were notably higher than those in the upstream catchment area and downstream gully bed of the other gullies with native grass. Comparatively, the flow rate and flow shear stress in the upstream catchment area of Gully 2 were lower than those in the upstream catchment areas of Gullies 1 and 4. In the downstream gully beds, the flow rate and flow shear stress in Gully 4 with native grass were lower than those in Gullies 1-3 with bare land.

As the experiment progressed, a fluctuating increasing trend in the flow rate was observed in the upstream catchment areas and downstream gully beds. At the initial stages, the flow rates ranged from 0.28 to 0.30 m s⁻¹, 0.19 to 0.21 m s⁻¹, 0.54 to 0.56 m s⁻¹, and 0.26 to 0.27 m s⁻¹ in the upstream catchment areas of Gullies 1, 2, 3 and 4, respectively. In addition, at the initial stages, the flow rates ranged from 0.50 to 0.52 m s⁻¹, 0.49 to 0.51 m s⁻¹, 0.54 to 0.55 m s⁻¹, and

Table 3 One-way ANOVA of the hydraulic properties of the upstream catchment areas of Gullies 1-4.

Item	Number (I)	Number (J)	Mean difference (I-J)	Standard error	P	95% confidence interval	
						Lower	Upper
Reynolds number	1	2	1252.83*	441.48	0.01	511.03	1994.62
		3	-11474.08*	441.48	0.01	-12215.87	-10732.29
		4	520.93	441.48	0.24	-220.86	1262.73
	2	3	-12726.91*	441.48	0.01	-13468.70	-11985.11
		4	-731.89*	441.48	0.10	-1473.69	9.90
	3	4	11995.02*	441.48	0.01	11253.22	12736.81
Froude number	1	2	0.05*	0.02	0.01	0.02	0.08
		3	-0.71*	0.02	0.01	-0.74	-0.68
		4	0.01	0.02	0.92	-0.03	0.03
	2	3	-0.75*	0.02	0.01	-0.78	-0.72
		4	-0.05*	0.02	0.01	-0.08	-0.02
	3	4	0.71*	0.02	0.01	0.68	0.74
Flow rate	1	2	0.10*	0.01	0.01	0.08	0.11
		3	-0.34*	0.01	0.01	-0.35	-0.32
		4	0.04*	0.01	0.01	0.03	0.06
	2	3	-0.44*	0.01	0.01	-0.45	-0.42
		4	-0.06*	0.01	0.01	-0.07	-0.04
	3	4	0.38*	0.01	0.01	0.36	0.39
Flow shear stress	1	2	0.29*	0.14	0.04	0.07	0.52
		3	-0.47*	0.14	0.01	-0.70	-0.24
		4	0.07	0.14	0.63	-0.16	0.30
	2	3	-0.77*	0.14	0.01	-1.00	-0.54
		4	-0.23	0.14	0.10	-0.46	0.00
	3	4	0.54*	0.14	0.01	0.31	0.77
Resistance <i>f</i>	1	2	-1.25*	0.14	0.01	-1.49	-1.01
		3	2.91*	0.14	0.01	2.67	3.15
		4	0.03	0.14	0.84	-0.21	0.27
	2	3	4.16*	0.14	0.01	3.92	4.40
		4	1.28*	0.14	0.01	1.04	1.52
	3	4	-2.88*	0.14	0.01	-3.12	-2.64
Flow energy consumption	1	2	-8.96*	1.40	0.01	-11.32	-6.60
		3	9.39*	1.40	0.01	7.03	11.75
		4	1.52	1.40	0.29	-0.84	3.88
	2	3	18.35*	1.40	0.01	15.99	20.70
		4	10.48*	1.40	0.01	8.12	12.84
	3	4	-7.87*	1.40	0.01	-10.23	-5.51

Note: * refers to $P \leq 0.1$.

0.39 to 0.41 m s⁻¹ in the downstream gully beds of Gullies 1, 2, 3 and 4, respectively. Following a period of landform adjustment, a steady-state flow rate was attained. The time-averaged steady-state flow rate values were 0.35, 0.23, 0.68, and 0.30 m s⁻¹ in the upstream catchment areas of Gullies 1-4 and 0.56, 0.54, 0.60, and 0.43 m s⁻¹ in the downstream gully beds of Gullies 1-4.

Similarly, a fluctuating increasing trend in the flow shear stress was also observed over time in the upstream catchment areas and downstream gully beds. At the initial stages, the flow shear stress in the upstream catchment areas and downstream gully beds was the most pronounced. Following an initial period of adjustment, steady-state flow shear stress conditions were attained in the upstream catchment areas and

downstream gully beds. The time-averaged steady-state flow shear stress values were 26.35, 26.49, 33.04, and 25.80 Pa in the upstream catchment areas of Gullies 1-4 and 55.11, 53.93, 60.16, and 47.83 Pa in the downstream gully beds of Gullies 1-4.

3.4 Changes in resistance *f* and flow energy consumption

Figs. 9 and 10 depict the variations in resistance *f* and flow energy consumption, respectively, in Gullies 1-4. Except for Gully 3, the values of resistance *f* in the upstream catchment areas were notably higher than those in the downstream gully beds in each gully. In addition, for Gullies 1 and 2, the flow energy consumption in the upstream catchment areas was

Table 4 One-way ANOVA of the hydraulic properties of the downstream gully beds of Gullies 1-4.

Item	Number (Gully I)	Number (Gully J)	Mean difference (I-J)	Standard error	P	95% confidence interval	
						Lower	Upper
Reynolds number	1	2	-295.60	354.83	0.41	-891.80	300.59
		3	-841.27*	354.83	0.02	-1437.46	-245.07
		4	1022.06*	354.83	0.01	425.86	1618.25
	2	3	-545.66	354.83	0.13	-1141.86	50.53
		4	1317.66*	354.83	0.01	721.47	1913.86
	3	4	1863.32*	354.83	0.01	1267.13	2459.52
Froude number	1	2	0.07*	0.03	0.01	0.03	0.12
		3	0.03	0.03	0.25	-0.01	0.08
		4	0.32*	0.03	0.01	0.28	0.37
	2	3	-0.04	0.03	0.13	-0.09	0.00
		4	0.25*	0.03	0.01	0.21	0.30
	3	4	0.29*	0.03	0.01	0.25	0.34
Flow rate	1	2	0.03*	0.01	0.01	0.02	0.05
		3	-0.02*	0.01	0.01	-0.03	-0.01
		4	0.13*	0.01	0.01	0.11	0.14
	2	3	-0.06*	0.01	0.01	-0.07	-0.04
		4	0.09*	0.01	0.01	0.08	0.11
	3	4	0.15*	0.01	0.01	0.14	0.16
Flow shear stress	1	2	0.18	0.21	0.40	-0.18	0.54
		3	-0.49*	0.21	0.03	-0.85	-0.13
		4	0.81*	0.21	0.01	0.45	1.17
	2	3	-0.67*	0.21	0.01	-1.03	-0.31
		4	0.63*	0.21	0.01	0.27	0.98
	3	4	1.29*	0.21	0.01	0.94	1.65
Resistance <i>f</i>	1	2	0.04	0.05	0.45	-0.05	0.12
		3	0.08	0.05	0.12	-0.01	0.17
		4	-1.10*	0.05	0.01	-1.18	-1.01
	2	3	0.04	0.05	0.43	-0.04	0.13
		4	-1.14*	0.05	0.01	-1.22	-1.05
	3	4	-1.18*	0.05	0.01	-1.26	-1.09
Flow energy consumption	1	2	0.67	1.53	0.67	-1.91	3.25
		3	0.26	1.53	0.87	-2.32	2.83
		4	-9.62*	1.53	0.01	-12.20	-7.04
	2	3	-0.41	1.53	0.79	-2.99	2.17
		4	-10.29*	1.53	0.01	-12.87	-7.71
	3	4	-9.88*	1.53	0.01	-12.46	-7.30

Note: * refers to $P \leq 0.1$.

notably higher than that in the downstream gully beds. However, the flow energy consumption in the upstream catchment area was notably lower than that in the downstream gully bed of Gully 4, containing native grass in both its upstream catchment area and downstream gully bed. In Gully 3, with bare land in the upstream catchment area and downstream gully bed, the resistance *f* and flow energy consumption values in the upstream catchment area were lower than those in the downstream gully bed.

As the experiment progressed, a fluctuating increasing trend in resistance *f* was observed in each gully. Except for the upstream catchment area of Gully 2, the resistance *f* in both the upstream catchment areas and downstream gully beds increased obviously at the initial stages. Following an

initial period of adjustment, steady-state resistance *f* conditions were attained in all treatments. In the upstream catchment area of Gully 2, resistance *f* decreased and then increased during the first 60 min. The time-averaged steady-state values of resistance *f* were 3.60, 5.27, 0.55, and 3.53 in the upstream catchment areas and 1.55, 1.51, 1.53, and 2.85 in the downstream gully beds of Gullies 1-4.

As the experiment progressed, the flow energy consumption increased logarithmically ($\Delta E = a + b \ln(t)$, $R^2 \geq 0.32$, $P \leq 0.05$) in the upstream catchment areas, headcuts, and downstream gully beds of each gully (Table 5). Rapid increases in flow energy consumption in the upstream catchment areas, headcuts and downstream gully beds occurred at the initial stages, and steady-state flow energy

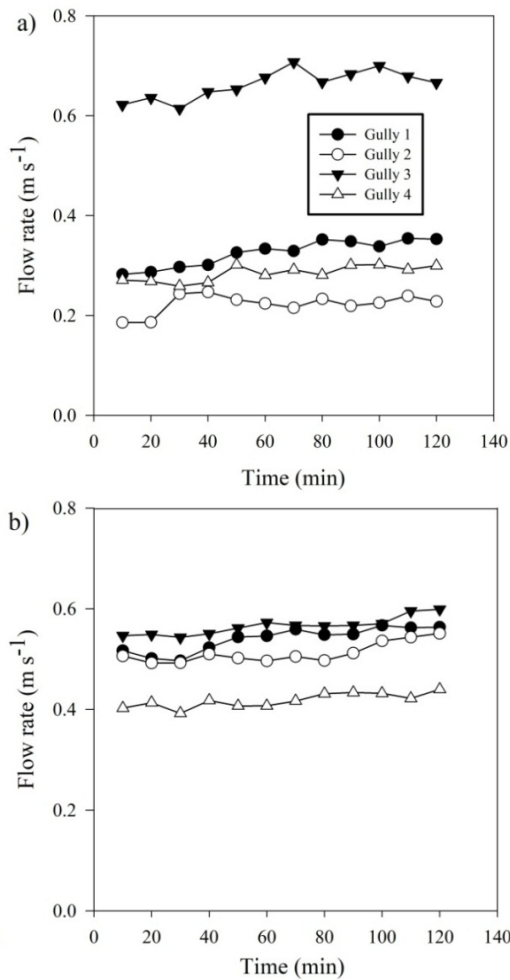


Fig. 7 Flow rate at the various gully positions in (a) the upstream catchment areas and (b) downstream gully beds over time.

consumption conditions were attained in all positions of the bank gullies. The time-averaged steady-state flow energy consumption values were estimated as follows: 38.79, 44.37, 27.17, and 34.77 $J s^{-1}$ in the upstream catchment areas; 18.27, 29.50, 16.18 and 19.58 $J s^{-1}$ in the headcuts; and 33.94, 32.16, 33.39 and 46.77 $J s^{-1}$ in the downstream gully beds of Gullies 1-4.

4 Discussion

4.1 Temporal variation in the erosion rate and hydraulic properties

Previous studies advocated that the active and stable stages were the two main developmental stages of gully evolution (Sidorchuk 1999). At the active gully stage (approximately 5% of the entire gully lifetime), erosion is intense, and the morphological

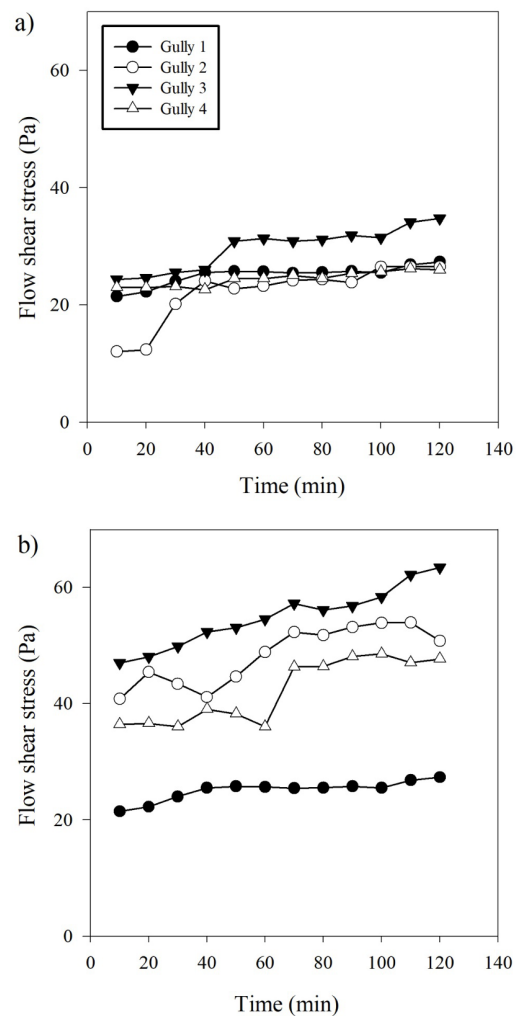


Fig. 8 Flow shear stress at the various gully positions in (a) the upstream catchment areas and (b) downstream gully beds over time.

characteristics are consequently far from constant, while in the remaining 95% of the gully lifetime, the morphologic conditions remain nearly stable (Sidorchuk 2006). In the present study, the sediment concentration in runoff was high and decreased rapidly at the initial stages. After a period of landform change (i.e., formation of shallow gullies in the upstream catchment and downstream gully bed) and infiltration adjustment, a relatively lower and stable sediment concentration in runoff was attained. Furthermore, although the setting of the experimental procedure and interruption of the experimental process would affect the steady state of the gully erosion process, the temporal variations in sediment concentration in runoff and infiltration rate would remain consistent, and a steady state of gully erosion could be achieved (Fig. 4b). This phenomenon is

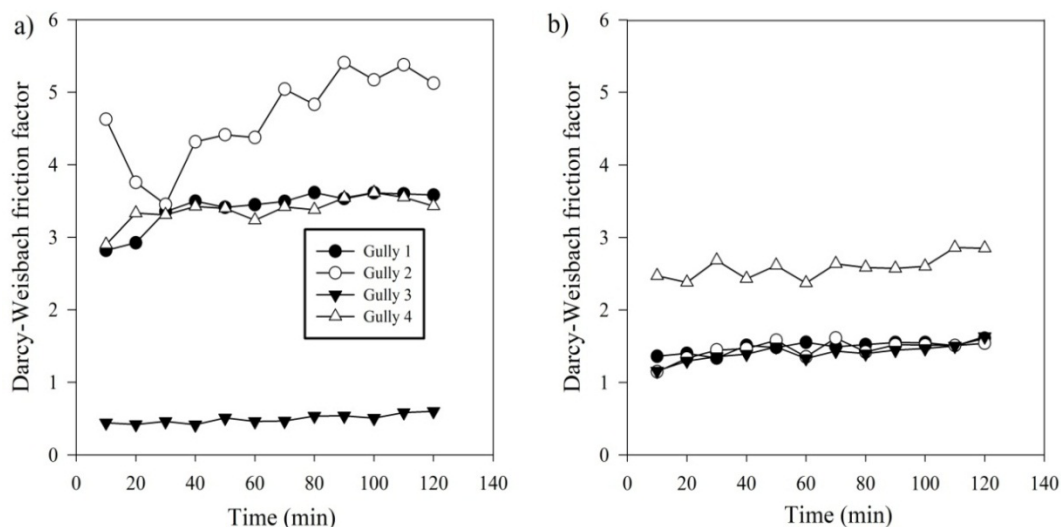


Fig. 9 Darcy-Weisbach friction factor at the various gully positions in (a) the upstream catchment areas and (b) downstream gully beds over time.

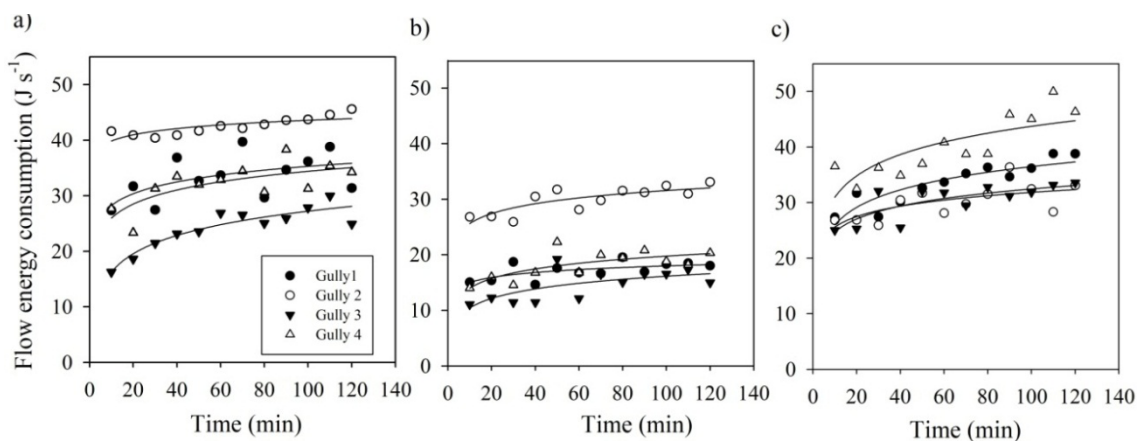


Fig. 10 Flow energy consumption at the various gully positions in (a) the upstream catchment areas, (b) gully walls and (c) downstream gully beds over time.

Table 5 Flow energy consumption ($J s^{-1}$) as a function of time (t) at each position in the four investigated gullies.

Item		Equation	R^2	F	P	N
Upstream catchment area	Gully 1	$\Delta E = 21.23 + 3.05 \ln(t)$	0.32	4.67	0.050	12
	Gully 2	$\Delta E = 36.11 + 1.62 \ln(t)$	0.59	14.55	0.003	12
	Gully 3	$\Delta E = 5.31 + 4.75 \ln(t)$	0.85	58.49	0.001	12
	Gully 4	$\Delta E = 17.55 + 3.65 \ln(t)$	0.52	10.95	0.008	12
Headcut	Gully 1	$\Delta E = 12.04 + 1.29 \ln(t)$	0.39	6.42	0.029	12
	Gully 2	$\Delta E = 19.67 + 2.58 \ln(t)$	0.66	19.07	0.001	12
	Gully 3	$\Delta E = 4.69 + 2.48 \ln(t)$	0.46	8.46	0.015	12
	Gully 4	$\Delta E = 8.23 + 2.50 \ln(t)$	0.54	11.82	0.006	12
Downstream gully bed	Gully 1	$\Delta E = 15.49 + 4.56 \ln(t)$	0.79	37.37	0.001	12
	Gully 2	$\Delta E = 19.37 + 2.70 \ln(t)$	0.44	7.87	0.018	12

attributable to the in situ flume experiment utilized, which would be significantly affected by weathering and soil cracking processes as a result of direct long-term exposure to sunlight under the special dry-hot conditions of the study area (Xiong et al. 2010; Su et al. 2015a). These results indicated that the soil

erosion rates not only rapidly changed at the initial stages and that relatively steady-state conditions were attained following the initial rapid variation period over the whole gully lifetime but also that similar changes in the soil erosion rates occurred during erosion events. Previous studies that were conducted

in the bank gullies of the in the dry-hot valley region of the Jinsha River of Southwest China at different flow discharges also reported similar results (Su et al. 2014; Dong et al. 2019). This result is also consistent with previous flume experiment studies (Bennett et al. 2000; Bennett and Casali 2001; Wells et al. 2009), which reported that a nearly invariant sediment discharge rate occurred after the initial stage of rapid gully development. In particular, it should be noted that a similar temporal variation in the generation of sediment could be found between treatments 1, 2 and 4 during the first 20 min due to native vegetation. These results were consistent with previous studies using in situ scouring experiments in this region (Yang et al. 2014; Dong et al. 2018). Furthermore, for gully 2, a lower and more steady state in sediment concentration in runoff was reached after 60-min scouring test than that after 20-min scouring test due to less fresh soil loss under high-density native grass as well as the interruption of the scouring experiment every 20 min. A previous study (Dong et al. 2018), which was conducted in five gully head plots containing different buffer strip widths with similar vegetation densities in the dry-hot valley region of the Jinsha River of Southwest China, also advocated that the effects of buffer strip width were remarkable on a relatively long time scale. The erosion processes in the bank gully would also be affected by some random processes during a single rainfall process, such as soil collapses at the headcuts and sidewall of the incision channels on gully beds due to gravity (Chen et al. 2013; Dong et al. 2019). Chen et al. (2013) revealed that the occurrence of the collapse of overhanging layers of the gully heads and sidewalls could be attributed to the development of a scour hole on the open side. For a long time scale, the sediment concentration at each plot showed similar decreasing trends. These results also indicated that the interruption of the scouring experiment would affect the soil erosion process, and more attention should be paid to this phenomenon.

Compared to the sediment concentration in runoff, the hydraulic properties also exhibited temporal variations across the bank gullies. Re , Fr , infiltration rate, flow rate, flow shear stress, resistance f and flow energy consumption showed a clear initial dynamic stage followed by a relatively stable stage throughout the 120-min gully erosion process as the experiment progressed. Accordingly, the temporal variations in the hydraulic properties,

such as Re and Fr , flow rate, flow shear stress, resistance f and energy consumption, could be ascribed to the temporal variations in the landform changes in the upstream catchment areas downstream gully beds of the bank gullies (Su et al. 2015a). A previous study conducted on the Loess Plateau of China reported similar results (Gong et al. 2011). Yang et al. (2015) also advocated that the hydraulic properties changed sharply in the early stage of the experiment and then tended to stabilize during 100-min situ scouring experiments for gully beds in the dry-hot valley region of the Jinsha River of Southwest China. Additionally, a converse temporal variation between sediment concentration in runoff and flow energy consumption could be found. This result could be ascribed to the increase in flow energy consumption per unit soil loss as the experiment progressed (Su et al. 2015a).

4.2 Spatial variation in the hydraulic properties

The Re value of the concentrated flow far exceeded 1000 under the experimental conditions, indicating that significant turbulent flow appeared in the upstream catchment areas and downstream gully beds of Gullies 1-4. This result is consistent with previous studies conducted in bank gullies in the dry-hot valley region of the Jinsha River of Southwest China (Su et al. 2015a; Dong et al. 2019). In the upstream catchment areas and downstream gully beds with native grass, Fr was lower than one, indicating that the concentrated flow was subcritical. Fr was higher than one in the upstream catchment areas and downstream gully beds with bare land at a flow discharge of 90 L min⁻¹, indicating that the concentrated flow was supercritical. These results were in agreement with the results of Dong et al. (2018). In addition, Fr in the upstream catchment area of Gully 3 was almost equal to that in its downstream gully bed, while Fr in the upstream catchment areas of the other three bank gullies was lower than those in their downstream gully beds. It should be noted that the slope of the downstream gully bed was notably higher than that of the upstream catchment area. These results indicated that the landform and native grass occurrence notably affected the concentration flow type.

The initial and steady-state flow rates in the downstream gully beds were notably higher than

those in the upstream catchment areas of Gullies 1, 2 and 4, while the resistance f values in the upstream catchment areas were notably higher than those in the downstream gully beds. Meanwhile, the initial and steady-state flow shear stress values in the downstream gully beds were notably higher than those in the upstream catchment areas of Gullies 1-4, which were consistent with the results of Su et al. (2015a, b), which were conducted in the dry-hot valley region of the Jinsha River of Southwest China. The flow energy consumption values in the upstream catchment areas were distinctly higher than those in the downstream gully beds of Gullies 1 and 2, while the initial and steady-state flow energy consumption values in the downstream gully beds were higher than those in the upstream catchment areas in Gullies 3 and 4. Furthermore, for Gully 4, two different species of vegetation were planted in the upstream catchment area and downstream gully bed, and these two different native grasses played similar roles in reducing hydraulics and sediment concentrations in runoff. These results indicated that a higher slope gradient could result in a higher flow rate and shear stress, while a higher native grass coverage could result in higher resistance f and flow energy consumption values and lower flow rate and shear stress levels. This result is consistent with previous studies (Yang et al. 2015; Dong et al. 2018), which were conducted in the dry-hot valley region of the Jinsha River of Southwest China and reported that grass buffer strips clearly decreased flow hydraulics (approximately 56%-70%) and increased flow resistance (1.2 to 1.5 times) according to the selected hydraulic parameters. Additionally, the different sizes of the upstream catchment area and downstream gully bed in bank gullies might also affect the hydraulics and soil erosion process of bank gullies and should be given more attention in future studies.

4.3 Impacts of native grass on erosion processes and hydraulic properties

Native grass could clearly decrease the sediment concentration in runoff by changing the flow type and increasing the soil infiltration rate. In the upstream catchment area, Re and Fr in Gully 3 with bare land were notably higher than those in the other three gullies, while Re and Fr in Gully 2 with two-year native grass were significantly lower than those in the other three gullies ($P < 0.1$, Table 2). No significant

differences in Re and Fr were observed between the upstream catchment areas of Gullies 1 and 4 ($P > 0.1$). Moreover, the Re and Fr values in the downstream gully bed of Gully 4 with native grass were significantly lower than those in the downstream gully beds of Gullies 1-3 with bare land ($P < 0.05$, Table 3). These results were consistent with previous studies (Yang et al. 2015; Dong et al. 2018), which were conducted in the dry-hot valley region of the Jinsha River of Southwest China and advocated that hydraulic parameters (i.e., Re and Fr) for the buffer strips (negative grass) were clearly smaller than those for the bare soil sites. Meanwhile, soil infiltration was higher in the gullies with negative grass than in those gullies with bare land. Previous studies also proposed that vegetation could increase flow resistance by intercepting runoff and increasing infiltration (Valentin et al. 2005; De Baets et al. 2011).

A previous study advocated that grass belts could play a positive role in reducing runoff shear stress and the soil erosion rate, enhancing the surface resistance and increasing flow energy consumption in bank gullies in the dry-hot valley region of the Jinsha River of Southwest China (Yang et al. 2015). In the present study, native grass also played an important role in decreasing the sediment concentration in runoff by reducing the flow rate and flow shear stress and increasing the surface roughness, resistance f and flow energy consumption. The resistance f and flow energy consumption values in the upstream catchment areas of Gully 3 with bare land were significantly lower than those in the other three gullies, while the resistance f and flow energy consumption values in Gully 2 with two-year native grass were notably higher than those in the other three gullies ($P < 0.1$, Table 2). No significant differences in the resistance f and flow energy consumption values were observed between the upstream catchment areas of Gullies 1 and 4 ($P > 0.1$). In the downstream gully beds, the resistance f and flow energy consumption values in Gully 4 with native grass were also notably higher than those gullies with bare land ($P < 0.1$, Table 3). These results indicated that the coverage and growth time of native grass could also effectively reduce the flow rate and flow shear stress and increase the surface roughness, resistance f and flow energy consumption. These results were also consistent with previous studies (Bastola et al. 2018; Dong et al. 2018). Yang et al. (2015) also reported that the reduction effectiveness

of runoff erosivity and sediment content may be strengthened as the distance between the gully headwall and grass belt decreases and the coverage of grass in the dry-hot valley region of the Jinsha River in Southwest China. Furthermore, for the headcuts, the flow energy consumption in Gully 2 was the highest and the flow energy consumption in Gully 3 was the lowest among Gullies 1-4. No clear difference in flow energy consumption was observed between the headcuts of Gullies 1 and 4. These results indicated that the flow energy consumption in the headcut was mainly influenced by the landform, vegetation coverage and hydraulic properties of the upstream catchment area in the bank gullies.

5 Conclusions

This study evaluated the effects of native grass on the sediment concentration in runoff and the hydraulic properties of bank gullies, and the results showed that native vegetation clearly reduced the sediment concentration in runoff and flow hydraulics (flow shear stress, flow rate and Fr) in bank gullies. Native grass is essential for erosion prevention in the upstream catchment areas and downstream gully beds of bank gullies because it plays an important role in reducing the Fr , flow rate and flow shear stress and increasing the infiltration rate, resistance f and flow energy consumption. Obvious temporal variations in the sediment concentration in runoff and hydraulic properties could also be observed in the bank gullies. At the initial stages, the soil erosion rate and

hydraulic properties, such as Re , Fr , infiltration rate, flow rate, flow shear stress, resistance f and flow energy consumption, in the upstream catchment areas and downstream gully beds were the most pronounced. Following an initial period of adjustment, steady-state soil erosion rates and hydraulic properties were attained in the bank gullies under the experimental conditions. Additionally, the sediment concentration in runoff and Fr exhibited decreasing trends over time under the experimental conditions, while Re , flow rate, flow shear stress, resistance f and flow energy consumption exhibited increasing trends as the experiments progressed. In further studies, more attention shall be paid to the temporal and spatial variability in the process of headcut erosion and the hydraulic characteristics of bank gullies for different vegetation measures.

Acknowledgements

This work was supported by the National Key Research and Development Program of China (2017YFC0505102), the Second Tibetan Plateau Scientific Expedition and Research Program (STEP, No. 2019QZKK0307), and the Major Science and Technology Program for Water Pollution Control and Treatment (2017ZX07101-001).

Electronic supplementary material: Supplementary materials (Appendixes 1, 2) are available in the online version of this article at <https://doi.org/10.1007/s11629-020-6287-9>.

References

- Bastola S, Dialynas YG, Bras RL, et al. (2018) The role of vegetation on gully erosion stabilization at a severely degraded landscape: A case study from Calhoun Experimental Critical Zone Observatory. *Geomorphology* 308: 25-39. <https://doi.org/10.1016/j.geomorph.2017.12.032>
- Bennett SJ, Casali J (2001) Effect of initial step height on headcut development in upland concentrated flows. *Water Resour Res* 37: 1475-1484. <https://doi.org/10.1029/2000WR900373>
- Bennett SJ, Casali J, Robinson KM, et al. (2000) Characteristics of actively eroding ephemeral gullies in an experimental channel. *T ASAE* 43: 641-649. <https://doi.org/10.13031/2013.2745>
- Chen A, Zhang D, Peng H, et al. (2013) Experimental study on the development of collapse of overhanging layers of gully in Yuanmou Valley, China. *Catena* 109: 177-185.
- De Baets S, Poesen J, Meersmans J, et al. (2011) Cover crops and their erosion-reducing effects during concentrated flow erosion. *Catena* 85: 237-244. <https://doi.org/10.1016/j.catena.2011.01.009>
- Dong YF, Xiong DH, Su ZA, et al. (2014) The distribution of and factors influencing the vegetation in a gully in the Dry-hot Valley of southwest China. *Catena* 116: 60-67. <https://doi.org/10.1016/j.catena.2013.12.009>
- Dong YF, Xiong DH, Su ZA, et al. (2013) Critical topographic threshold of gully erosion in Yuanmou Dry-hot Valley in Southwestern China. *Phys Geogr* 34: 50-59. <https://doi.org/10.1080/02723646.2013.778691>
- Dong YF, Xiong DH, Su ZA, et al. (2018) Effects of vegetation buffer strips on concentrated flow hydraulics and gully bed erosion based on in situ scouring experiments. *Land Degrad Dev* 29: 1672-1682. <https://doi.org/10.1002/ldr.2943>
- Dong YF, Xiong DH, Su ZA, et al. (2019) The influences of mass failure on the erosion and hydraulic processes of gully headcuts based on an in situ scouring experiment in Dry-hot valley of China. *Catena* 176: 14-25. <https://doi.org/10.1016/j.catena.2019.01.004>
- FAO (2015) World reference base for soil resources 2014. International soil classification system for naming soils and creating legends for soil maps. World Soil Resources Report 106, Rome.
- Fu B, Liu Y, Lü Y, et al. (2011) Assessing the soil erosion control service of ecosystems change in the Loess Plateau of China. *Ecol Complexity* 8: 284-293.

- <https://doi.org/10.1016/j.ecocom.2011.07.003>
 Gómez Gutiérrez Á, Schnabel S, Felicísimo ÁM (2009) Modelling the occurrence of gullies in rangelands of southwest Spain. *Earth Surf Proc Land* 34: 1894-1902.
<https://doi.org/10.1002/esp.1881>
- Gong JG, Jia YW, Zhou ZH, et al. (2011) An experimental study on dynamic processes of ephemeral gully erosion in loess landscapes. *Geomorphology* 125: 203-213.
<https://doi.org/10.1016/j.geomorph.2010.09.016>
- Gudino-Elizondo N, Biggs TW, Castillo C, et al. (2018) Measuring ephemeral gully erosion rates and topographical thresholds in an urban watershed using unmanned aerial systems and structure from motion photogrammetric techniques. *Land Degrad Dev* 29: 1896-1905.
<https://doi.org/10.1002/ldr.2976>
- Hancock GR, Evans KG (2006) Gully position, characteristics and geomorphic thresholds in an undisturbed catchment in Northern Australia. *Hydrol Process* 20: 2935-2951.
<https://doi.org/10.1002/hyp.6085>
- Hancock GR, Evans KG (2010) Gully, channel and hillslope erosion – an assessment for a traditionally managed catchment. *Earth Surf Proc Land* 35: 1468-1479.
<https://doi.org/10.1002/esp.2043>
- Horton RE (1945) Erosional development of streams and their drainage basins: hydrophysical approach to quantitative morphology. *Bulletin of the Geological Society of America* 56: 275-370. [https://doi.org/10.1130/0016-7606\(1945\)56\[275:EDOSAT\]2.o.CO;2](https://doi.org/10.1130/0016-7606(1945)56[275:EDOSAT]2.o.CO;2)
- Kirkby MJ, Bull LJ, Poesen J, et al. (2003) Observed and modelled distributions of channel and gully heads - with examples from SE Spain and Belgium. *Catena* 50: 415-434.
[https://doi.org/10.1016/S0341-8162\(02\)00128-5](https://doi.org/10.1016/S0341-8162(02)00128-5)
- Marzloff I, Ries JB, Poesen J (2011) Short-term versus medium-term monitoring for detecting gully erosion variability in a Mediterranean environment. *Earth Surf Proc Land* 36: 1604 - 1623. <https://doi.org/10.1002/esp.2172>
- Nyssen J, Veyret-Picot M, Poesen J, et al. (2004) The effectiveness of loose rock check dams for gully control in Tigray, northern Ethiopia. *Soil Use Manage* 20: 55-64.
<https://doi.org/10.1111/j.1475-2743.2004.tb00337.x>
- Pederso, JL, Petersen PA, Dierker JL (2006) Gullying and erosion control at archaeological sites in Grand Canyon, Arizona. *Earth Surf Proc Land* 31: 507-525.
<https://doi.org/10.1002/esp.1286>
- Poesen J, Nachtergaele J, Verstraeten G, et al. (2003) Gully erosion and environmental change: importance and research needs. *Catena* 50: 91-133.
[https://doi.org/10.1016/S0341-8162\(02\)00143-1](https://doi.org/10.1016/S0341-8162(02)00143-1)
- Shellberg JG, Spencer J, Brooks AP, et al. (2016) Degradation of the Mitchell River fluvial megafan by alluvial gully erosion increased by post-European land use change, Queensland, Australia. *Geomorphology* 266: 105-120.
<https://doi.org/10.1016/j.geomorph.2016.04.021>
- Sidorchuk A (1999) Dynamic and static models of gully erosion. *Catena* 37: 401-414.
[https://doi.org/10.1016/S0341-8162\(99\)00029-6](https://doi.org/10.1016/S0341-8162(99)00029-6)
- Sidorchuk A (2006) Stages in gully evolution and self-organized criticality. *Earth Surf Proc Land* 31: 1329-1344.
<https://doi.org/10.1002/esp.1334>
- Su ZA, Xiong DH, Zhang JH, et al. (2019) Variation in the vertical zonality of erodibility and critical shear stress of rill erosion in China's Hengduan Mountains. *Earth Surf Proc Land* 44: 88-97. <https://doi.org/10.1002/esp.4482>
- Su ZA, Xiong DH, Dong YF, et al. (2014) Simulated headward erosion of bank gullies in the Dry-hot Valley Region of southwest China. *Geomorphology* 204: 532-541.
<https://doi.org/10.1016/j.geomorph.2013.08.033>
- Su ZA, Xiong DH, Dong YF, et al. (2015a) Hydraulic properties of concentrated flow for a bank gully in the Dry-hot Valley Region of southwest China. *Earth Surf Proc Land* 40: 1351-1363. <https://doi.org/10.1002/esp.3724>
- Su ZA, Xiong DH, Dong YF, et al. (2015b) Influence of bare soil and cultivated land use types upstream of a bank gully on soil erosion rates and energy consumption for different gully erosion zones in the dry-hot valley region, Southwest China. *Nat Hazards* 79: S183-S202.
<https://doi.org/10.1007/s11069-015-1722-x>
- Tebebu TY, Abiy AZ, Zegeye AD, et al. (2010) Surface and subsurface flow effect on permanent gully formation and upland erosion near Lake Tana in the northern highlands of Ethiopia. *Hydrol Earth Syst Sc* 14: 2207-2217.
<https://doi.org/10.5194/hess-14-2207-2010>
- Valentin C, Poesen J, Li Y (2005) Gully erosion: Impacts, factors and control. *Catena* 63: 132-153.
<https://doi.org/10.1016/j.catena.2005.06.001>
- Vandekerckhove L, Poesen J, Wijdenes DO, et al. (1998) Topographical thresholds for ephemeral gully initiation in intensively cultivated areas of the Mediterranean. *Catena* 33: 271-292. [https://doi.org/10.1016/S0341-8162\(98\)00068-X](https://doi.org/10.1016/S0341-8162(98)00068-X)
- Wells RR, Alonso CV, Bennett SJ (2009) Morphodynamics of headcut development and soil erosion in upland concentrated flows. *Soil Sci Soc Am J* 73: 521-530.
<https://doi.org/10.2136/sssaj2008.0007>
- Wells RR, Bennett SJ, Alonso CV (2010) Modulation of headcut soil erosion in rills due to upstream sediment loads. *Water Resour Res* 46. <https://doi.org/10.1029/2010.WR009433>
- Wells RR, Momm HG, Bennett SJ, et al. (2016) A Measurement Method for Rill and Ephemeral Gully Erosion Assessments. *Soil Sci Soc Am J* 80: 203-214.
<https://doi.org/10.2136/sssaj2015.09.0320>
- Wilkinson SN, Hancock GJ, Rebecca B, et al. (2013) Using sediment tracing to assess processes and spatial patterns of erosion in grazed rangelands, Burdekin River basin, Australia. *Agric Ecosyst Environ* 180: 90-102.
<https://doi.org/10.1016/j.agee.2012.02.002>
- Wilson G (2011) Understanding soil-pipe flow and its role in ephemeral gully erosion. *Hydrol Process* 25: 2354-2364.
<https://doi.org/10.1002/hyp.7998>
- Xiong DH, Yan D, Long Y, et al. (2010) Simulation of morphological development of soil cracks in Yuanmou Dry-hot Valley Region, Southwest China. *Chinese Geogr Sci* 20: 112-122.
- Yang D, Xiong DH, Guo M, et al. (2014) Impact of grass belt position on the hydraulic properties of runoff in gully beds in the Yuanmou Dry-hot Valley Region of Southwest China. *Phys Geogr* 36: 408-425.
<https://doi.org/10.1080/02723646.2015.1074517>
- Yang D, Xiong DH, Guo M, et al. (2015) Impact of grass belt position on the hydraulic properties of runoff in gully beds in the Yuanmou Dry-hot valley region of Southwest China. *Phys Geogr* 36: 408-425.
- Zabihi M, Mirchooli F, Motevalli A, et al. (2018) Spatial modelling of gully erosion in Mazandaran Province, northern Iran. *Catena* 161: 1-13.
<https://doi.org/10.1016/j.catena.2017.10.010>
- Zakerinejad R, Maerker M (2015) An integrated assessment of soil erosion dynamics with special emphasis on gully erosion in the Mazayjan basin, southwestern Iran. *Nat Hazards* 791: S25-S50. <https://doi.org/10.1007/s11069-015-1700-3>
- Zegeye AD, Langendoen EJ, Tilahun SA, et al. (2018) Root reinforcement to soils provided by common Ethiopian highland plants for gully erosion control. *Ecology* 11: UNSP e1940. <https://doi.org/10.1002/eco.1940>
- Zhang BJ, Xiong DH, Zhang GH, et al. (2018) Impacts of headcut height on flow energy, sediment yield and surface landform during bank gully erosion processes in the Yuanmou Dry-hot Valley region, southwest China. *Earth Surf Proc Land* 43: 2271-2282. <https://doi.org/10.1002/esp.4388>
- Zhu TX (2012) Gully and tunnel erosion in the hilly Loess Plateau region, China. *Geomorphology* 153: 144-155.
<https://doi.org/10.1016/j.geomorph.2012.02.019>